Bioorganic Chemistry 112 (2021) 104836

Contents lists available at ScienceDirect

Bioorganic Chemistry

journal homepage: www.elsevier.com/locate/bioorg

A novel β-hairpin peptide derived from the ARC repressor selectively interacts with the major groove of B-DNA

Azzurra Stefanucci [a,1], Jussara Amato [b,1], Diego Brancaccio [b], Bruno Pagano [b], Antonio Randazzo [b], Federica Santoro [b], Laura Mayol [b], Soraya Learte-Aymamí [c], Jessica Rodriguez [c], José Luis Mascareñas [c], Ettore Novellino [b], Alfonso Carotenuto [b,*], Adriano Mollica [a,*]

[a] Department of Pharmacy, University of Chieti-Pescara "G. d'Annunzio", Via dei Vestini 31, 66100 Chieti, Italy
[b] Department of Pharmacy, University of Naples "Federico II", Via D. Montesano 49, 80131 Naples, Italy
[c] Centro Singular de Investigación en Química Biolóxica e Materiais Moleculares (CIQUS), and Departamento de Química Orgánica. Universidade de Santiago de Compostela, 15782 Santiago de Compostela, Spain

ARTICLE INFO

Keywords:
Transcription factors
ARC repressor
DNA major groove binders
β-hairpin peptides
Conformational analysis

ABSTRACT

Transcription factors (TFs) have a remarkable role in the homeostasis of the organisms and there is a growing interest in how they recognize and interact with specific DNA sequences. TFs recognize DNA using a variety of structural motifs. Among those, the ribbon-helix-helix (RHH) proteins, exemplified by the MetJ and ARC repressors, form dimers that insert antiparallel β-sheets into the major groove of DNA. A great chemical challenge consists of using the principles of DNA recognition by TFs to design minimized peptides that maintain the DNA affinity and specificity characteristics of the natural counterparts. In this context, a peptide mimic of an antiparallel β-sheet is very attractive since it can be obtained by a single peptide chain folding in a β-hairpin structure and can be as short as 14 amino acids or less. Herein, we designed eight linear and two cyclic dodeca-peptides endowed with β-hairpins. Their DNA binding properties have been investigated using fluorescence spectroscopy together with the conformational analysis through circular dichroism and solution NMR. We found that one of our peptides, peptide **6**, is able to bind DNA, albeit without sequence selectivity. Notably, it shows a topological selectivity for the major groove of the DNA which is the interaction site of ARC and many other DNA-binding proteins. Moreover, we found that a type I' β-hairpin folding pattern is a favorite peptide structure for interaction with the B-DNA major groove. Peptide **6** is a valuable lead compound for the development of novel analogs with sequence selectivity.

1. Introduction

Gene transcription is regulated by transcription factors (TFs) which bind to operator DNA, influencing the ability of RNA polymerase to initiate transcription. In eukaryotic organisms, protein transcription stands at the beginning of the process by interplay among multiple general transcription factors, activators/repressors, mediator/coactivators, multiple regulatory sequences (proximal and distant), chromatin and its impact on transcription, co-transcriptional RNA processing, regulation of transcriptional regulators [1].

Although TFs recognize DNA using a variety of structural motifs, in many cases they share similar structural recognition motifs, which facilitate a classification into families [2,3]. In many of these families the most relevant contacts to DNA occur in the major groove from amino acids of α-helical regions, known as recognition helices, embedded in those motifs. Among those, there are the bihelical DNA-binding motif (helix-turn-helix), zinc-finger domains, and the basic region-leucine zipper (bZIP) motif.

In addition to the above motifs, there are TFs and other DNA-binding proteins that do not rely on α-helices for specific DNA recognition, although they are less common. For instance, the ribbon-helix-helix (RHH) proteins, exemplified by the MetJ and ARC repressors, form

* Corresponding authors.
E-mail addresses: alfonso.carotenuto@unina.it (A. Carotenuto), a.mollica@unich.it (A. Mollica).
[1] These two authors contributed equally.

https://doi.org/10.1016/j.bioorg.2021.104836
Received 22 May 2020; Received in revised form 4 February 2021; Accepted 17 March 2021
Available online 22 March 2021

dimers that insert antiparallel β-sheets into the major groove of DNA with the side chains on the face of the β-sheet contacting the base pairs.

Taking into account the great importance of TFs role in the homeostasis of the organisms, there is a growing interest in how TFs recognize and interact with specific DNA sequences. It is well known that aberrant recognition properties of some proteins stand at the origin of several diseases such as cancer, prion diseases, and muscular Duchenne dystrophy [4–6].

Therefore, the molecular basis of their supramolecular behaviors is a hot topic in biochemistry, as well as in medicinal chemistry for the development of non-natural DNA binding protein mimetics.

ARC is a protein commonly expressed at low levels from the phage. Solution properties of ARC repressors (wild-type and F10H variant) from Salmonella bacteriophage P22 and their complexes with operator DNA were described by Dostál et al. by circular dichroism, fluorescence, and Raman difference spectroscopy and compared with the crystal structures of free and DNA-bound ARC repressors (wild-type and F10V variant) [7]. Data indicate that the binding of ARC in the major groove of the DNA involves hydrogen bonds of amino acid residues with DNA nucleobases, together with slight perturbations of the deoxyribose ring systems. Furthermore, the key residue Trp14 of ARC repressor monomer acts as a sensitive probe for modifications of the hydrophobic core of the protein [7].

Building synthetic ARC mimetics able to recognize specific double stranded DNA (ds-DNA) and the design of small molecules capable to control ARC activity, could be valuable approaches in medicinal chemistry [8].

A great chemical challenge consists of using the principles of DNA recognition by TFs to design minimized peptides that maintain the DNA affinity and specificity characteristics of the natural counterparts [9,10].

Recently, we described the first synthetic analogue of ARC repressor as β-sheet mimetic peptide based on the structural moiety of the native protein. This novel entity was able to bind both the DNA sequence containing the consensus target (TAGA) and one with a double mutation in the consensus sequence, deceiving the expecting specificity for the consensus target site [11]. In this context, a peptide mimic of an antiparallel β-sheet is very attractive since it can be obtained by a single peptide chain folding in a β-hairpin structure and can be as short as 14 amino acids or less [12].

Herein, with the aim to discover biomimetic peptides of ARC repressor able to recognize specific sequences on the DNA major groove, we designed eight linear and two cyclic dodeca-peptides (Table 1) endowed with β-hairpins. β-hairpin structures promote the protein folding through the participation in hydrophobic core's formation, providing a scaffold for the building of more complex structures, so as they can be considered as the simplest model of a β-sheet structure [13].

The DNA binding properties have been investigated using fluorescence spectroscopy and anisotropy assay together with the peptide conformational analysis through circular dichroism (CD) and solution NMR. Molecular docking calculations were also carried out to disclose atomic details of the binding.

Table 1
Amino acid sequences of the novel synthetic peptides.

Structure Type	Compounds	Sequences[a]
β-sheet portion	**ARC protein**	**P-Q-F-N-L-R-W-P//P-Q-F-N-L-R-W-P**
Linear β-hairpins	**1**	**Q-F-N-L-R-***N-G***-Q-F-N-L-R**-NH_2
	2	**Q-F-N-L-R-***G-N***-Q-F-N-L-R**-NH_2
	3	**Q-F-N-L-R-***p-P***-Q-F-N-L-R**-NH_2
	4	**Q-F-N-L-R-***P-p***-Q-F-N-L-R**-NH_2
	5	**Q**-W-**N**-W-**R-***N-G***-Q**-W-**N**-W-**R**-NH_2
	6	**Q**-W-**N**-W-**R-***G-N***-Q**-W-**N**-W-**R**-NH_2
	7	**Q**-W-**N**-W-**R-***p-P***-Q**-W-**N**-W-**R**-NH_2
	8	**Q**-W-**N**-W-**R-***P-p***-Q**-W-**N**-W-**R**-NH_2
Cyclic β-hairpins	**9**	**Q-F-N-***c*[**CR-***N-G***-QC**]**N-L-R**-NH_2
	10	**Q-***c*[**CNLR-***N-G***-QFNC**]**R**-NH_2

[a] Lower case letter indicates D-amino acids. In bold are shown the conserved natural residues. In italics are shown the β-turn inducers.

2. Materials and methods

2.1. Chemicals

Calf thymus DNA, EB, MG, and H33258 dyes were purchased from Sigma Aldrich (Merck Group). Each dye was dissolved as a concentrated stock solution (~5 mg/mL) in H_2O, and serial dilutions were made from this stock. Concentrations of the dyes were determined in H_2O using the following extinction coefficients supplied by Molecular Probes: EB = 5.5 × 10^3 M^{-1} cm^{-1} (546 nm); MG = 85.3 × 10^3 M^{-1} cm^{-1} (638 nm). The concentration of H33258 was determined in methanol using the extinction coefficient of 46 × 10^3 M^{-1} cm^{-1} (344 nm). DNA1 (5′-GCGAGTAGAGCTTTTTGCTCTACTCGC-3′) and DNA2 (5′-GCGAGCA-CAGCTTTTTGCTGTGCTCGC-3′) oligomers were provided from Biomers (Germany) and used without further purification. DNAs were dissolved in 10 mM Tris-HCl buffer (pH 7.4) and then annealed to allow the formation of their corresponding hairpin structures [14]. Peptides **1**–**10** were purchased from China Peptides (Shangai, China). They were analyzed by analytical RP-HPLC and ESI-MS to assess their purity and to confirm chemical identity (Supplementary Material, Table S1).

2.2. Circular dichroism (CD)

CD spectra were carried out on a Jasco-715 coupled with a thermostat Nestlab RTE-11, using an acquisition range: 250–190 nm; band width: 2.0 nm; resolution: 0.2 nm; accumulation: 3 scans; sensitivity: 10 mdeg; response time: 0.25 s, speed: 100 nm/min. CD measurements were made in a 2 mm cell at 20 °C. Peptides **1**–**10** (125 μM) were dissolved in 10 mM phosphate buffer (pH 7.5) containing 100 mM of NaCl.

2.3. NMR spectroscopy

The samples for NMR spectroscopy were prepared by dissolving the appropriate amount of peptide **2**, **3**, **4**, **6**, or **8** in 0.18 mL of H_2O and 0.02 mL of ^2H_2O (pH 5.5), to obtain a concentration 1 mM in peptide solution. NMR spectra were recorded on a Varian INOVA 700 MHz spectrometer equipped with a z-gradient 5 mm triple-resonance probe head. All the spectra were recorded at a temperature of 25 °C. One-dimensional (1D) NMR spectra were recorded in the Fourier mode with quadrature detection. The water signal was suppressed by gradient echo [15]. 2D DQF-COSY [16–18], TOCSY [19], and NOESY [20] spectra were recorded in the phase-sensitive mode using the method from States [21]. Data block sizes were 2048 addresses in t_2 and 512 equidistant t_1 values. Before Fourier transformation, the time domain data matrices were multiplied by shifted sin^2 functions in both dimensions. A mixing time of 80 ms was used for the TOCSY experiments. NOESY experiments were run with a mixing time of 100 ms. The qualitative and quantitative analyses of DQF-COSY, TOCSY, and NOESY spectra, were obtained using the interactive program package XEASY [22]. Almost complete ^1H NMR chemical shift assignments were effectively achieved for all peptides according to the Wüthrich [18] procedure via the usual systematic application of DQF-COSY, TOCSY, and NOESY experiments with the support of the XEASY software package (Supplementary Material, Tables S2–S6).

2.4. Structure calculation

The NOE-based distance restraints were obtained from NOESY spectra of peptide **6**. The NOESY cross peaks were integrated with the XEASY program and were converted into upper distance bounds using the CALIBA program incorporated into the program package CYANA [23]. Only NOE derived constraints were considered in the annealing procedures. An ensemble of 100 structures was generated with the simulated annealing of the program CYANA. Then, 10 structures were

chosen, whose interproton distances best fitted NOE derived distances, and refined through successive steps of restrained and unrestrained energy minimization calculations using the Discover algorithm (Accelrys, San Diego, CA) and the consistent valence force field [24]. The minimization lowered the total energy of the structures; no residue was found in the disallowed region of the Ramachandran plot. The final structures were analyzed using the InsightII program (Accelrys, San Diego, CA). Molecular graphics images were realized using the UCSF Chimera package [25].

2.5. Methyl green displacement assay

Methyl Green (MG) displacement experiments were performed at 20 °C on a FP-8300 spectrofluorometer (Jasco) equipped with a Peltier temperature controller accessory (Jasco PCT-818). A sealed quartz cuvette with a path length of 1 cm was used. Fluorescence spectra were recorded with excitation at 640 nm and emission from 645 to 750 nm. Excitation and emission slits were set both at 5 nm. For the assay 8.2 μg/mL (1 μM single strand, or 27 μM per nucleotide) of pre-folded DNA1 or DNA2 targets and 100 μg/mL (312 μM per nucleotide) CT-DNA were used. DNA/MG solutions were prepared by mixing each DNA with MG (1.26 μM in the case of DNA1 and DNA2 or 15.3 μM for CT), and the corresponding mixtures were stirred at room temperature for 1 h before use. The ability of peptides **2**, **3**, **4**, **6**, and **8** to displace MG from DNA1, DNA2 was evaluated by adding each peptide to a final concentration of 35 μM (450 μM for CT). Stock solutions of peptides were prepared in ultra-pure H_2O at a concentration of 2 mM. All DNA/MG/peptide mixtures were equilibrated for 3 min before spectra acquisition.

For the displacement titration, different amounts of peptide **6** (from a 20 mM stock solution) were added to the DNA/MG solution (from 0 to 78 μM in the case of DNA1, from 0 to 39 μM for DNA2, and from 0 to 423 μM in the case of CT) followed by a 3 min equilibration time before spectra acquisition. The percentage of displacement was calculated as follows: MG displacement (%) = 100 − [(F/F_0) × 100], where F stands for the intensity of the fluorescence emission signal at 660 nm of MG bound to DNA after each ligand addition and F_0 without added ligand. The percentage of displacement was then plotted as a function of the concentration of added ligand. DC_{50} values were designed as the required concentration to displace 50% MG from each investigated DNA.

2.6. Hoechst 33258 displacement assay

Hoechst 33258 (H33258) displacement experiments were performed as already reported for MG, except for the fact that fluorescence emission spectra were recorded in the 350–650 nm range upon excitation at 344 nm. For each assay 3 μg/mL (0.37 μM single strand, or 10 μM per nucleotide) of pre-folded DNA1 or DNA2 targets and 1 μg/mL (1.87 μM) of H33258 were used, and the corresponding DNA/H33258 mixtures were stirred at room temperature for 1 h before use. Next, each peptide (**2**, **3**, **4**, **6**, and **8**) was added to the corresponding DNA/dye solution to a final concentration of 56 μM. Stock solutions of peptides were 2 mM in ultra-pure H_2O.

2.7. Ethidium bromide displacement assay

Ethidium bromide (EB) displacement spectra were obtained with a Jobin-Yvon Fluoromax-3 (DataMax 2.20) coupled to a Wavelength Electronics LFI-3751 temperature controller, using the following settings: increment: 1.0 nm; integration time: 0.1 s; excitation slit width: 4.0 nm; emission slit width: 6.0 nm at 20 °C. In the case of ethidium bromide, the excitation wavelength applied was 540 nm and the emission spectra were acquired from 565 to 650 nm. For each assay 1 μM of pre-folded DNA1 or DNA2 targets and 4.5 μM of EB were used, and the corresponding DNA/EB mixtures were stirred at room temperature for 1 h before use. Next, each peptide (**2**, **3**, **4**, **6**, and **8**) was added to the corresponding DNA/dye solution to a final concentration of 15 μM. Stock solutions of peptides were 2 mM in ultra-pure H_2O.

2.8. Anisotropy assay

Measurements were made with a Jobin-Yvon Fluoromax-3, (DataMax 2.20) coupled to a Wavelength Electronics LFI − 3751 temperature controller, using a Hellma micro cuvette of 1 mL. Settings: integration time: 2.0 s; excitation slit width: 5.0 nm; emission slit width: 20.0 nm; excitation wavelength 559 nm; emission wavelength 585 nm. For each assay, 1 μM of pre-folded tetramethylrhodamine (TMR)-DNA1 or TMR-DNA2 (5 μL, 100 μM) was added to 495 μL of Tris-HCl buffer 20 mM pH 7.5, 100 mM NaCl, and the anisotropy was measured. Aliquots of a stock solution in ultra-pure H_2O (1 mM) of the peptide **6** were successively added to this solution, and the anisotropic value was recorded after each addition.

Experimental data were fitted with the *DynaFit 4.0* software, which performs a numerical treatment of the system [26,27]. The program is available free of charge for academia at *http://www.biokin.com/dynafit/*.

2.9. Viscosity study

Viscosity of CT-DNA (50 μM) in the Tris-HCl buffer solution (pH = 7.4) was measured in absence (η_o) or presence (η_P) of the peptide **6** in order to evaluate the effect of peptide **6** addition on CT-DNA solution viscosity as a consequence of their interactions. Peptide concentration was varied to obtain a concentration ratio ($r = \frac{C_{CT-DNA}}{C_p}$) equal to 0.1, 0.6, 1.2 and 1.5. Viscosity measurements were performed by shear experiments using a rotational rheometer (MalvernKinexus), equilibrated at 20 °C. Shear viscosity values of the solutions were recorded at fixed shear rate values equal to 0.1, 1 and 10 s^{-1}.

2.10. Docking study

DNA1 and DNA2 models were built in B-DNA conformation using the Biopolymer tool of the InsightII program (Accelrys, San Diego). Only the double helix segments of the oligonucleotides were included in the models (bases 1–11 and 17–27). The poses for the **6**/DNA complex were generated by docking the lowest energy conformers of peptide **6** obtained by NMR to the DNA1 and DNA2 models using the program AUTODOCK 4.2 [28]. Docking statistics are reported in Table S7 of the Supplementary Material. Refinement of lowest energy pose of both **6**/DNA1 and **6**/DNA2 complexes was achieved by *in vacuo* energy minimization with the Discover algorithm using the steepest descent and conjugate gradient methods until a RMSD of 0.05 kcal/mol per Å was reached. Energy terms in Table S7 refer to these optimized complexes.

3. Results and discussion

3.1. Design

In the design of the novel β-hairpin peptides we explored different types of structural modifications involving the native amino acid sequence of the ARC protein, primarily by conserving the key amino acids of each β-strand (*e.g.* QFNLR) to guarantee the sequence specific interactions with the DNA. A series of well-known dipeptide β-turn inducers have been incorporated between the two strands in place of Trp-Pro sequence, to promote the β-hairpin formation (Fig. 1) [29].

A β-turn is a stable pseudo cyclic secondary structure, made of 10 atoms, and formed by four residues, where the second and third residues have a key role in the folding of the peptide [30]. Only specific dipeptide sequences are able to induce and stabilize the formation of a β-turn structure [29]. Once a β-turn is formed and stabilized by an intramolecular H-bond, it is capable to fold a peptide into a β-hairpin structure [31].

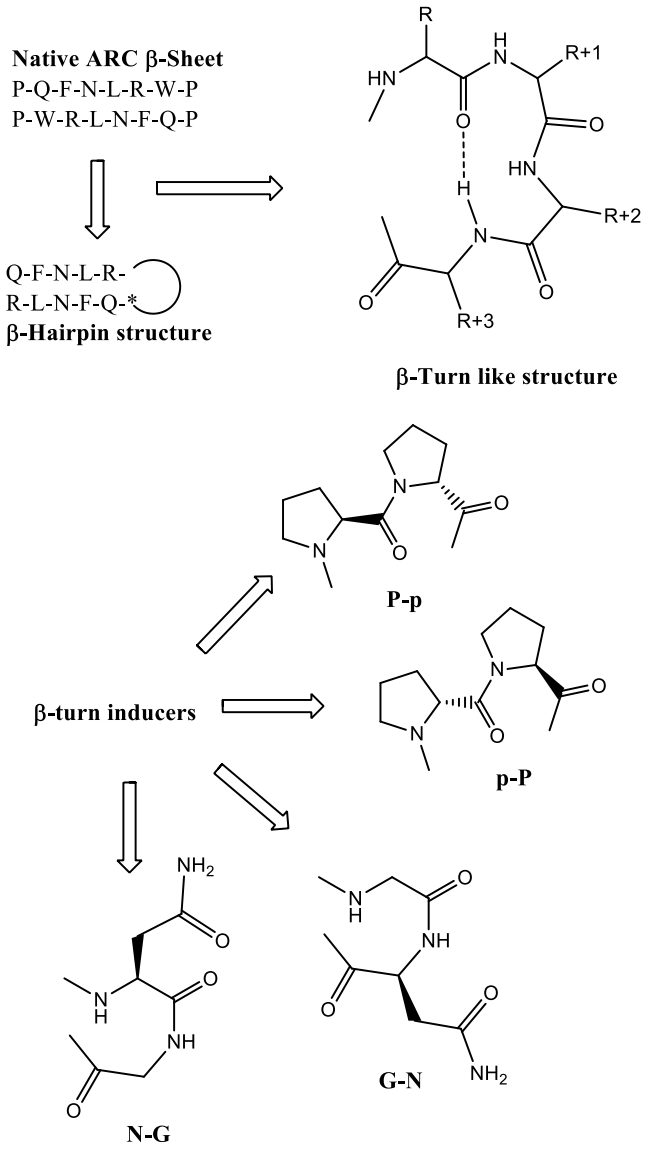

Fig. 1. Native ARC β-sheet and β -turn inducer sequences incorporated in the novel peptides.

In particular, Asn-Gly (*N*-G) dipeptide is a type I' β-turn and Gly-Asn (G-N) dipeptide is a type II' β-turn inducer [12]. Also, DPro-Pro (p-P) has been used as nucleating turn of β-hairpins promoting a type II′ β-turn [32]. Furthermore, the enantiomeric Pro-DPro (P-p) sequence was attempted. One-by-one insertion of these four dipeptide β-turn inducers gave peptides **1**–**4** reported in Table 1. Then, considering that in the crystal structure of ARC repressor in complex with its DNA target site (PDB: 1PAR), Phe and Leu residues are buried into the protein hydrophobic core, they were replaced with Trp residues in all peptides **1**–**4** to obtain a Trp-Zip like structure [33], resulting in compounds **5**–**8**, respectively (Table 1). To further force the folding of the Asn-Gly β-turn containing peptides into a β-hairpin secondary structure, two cysteine residues have been inserted in place of the faced residues Leu and Phe [7], in order to close the cycle by a disulfide bridge. In this way two novel constrained peptides have been obtained (compounds **9**–**10**). All the original sequences have been prepared as *C*-terminal amide to avoid undesirable unspecific ionic interactions with DNA.

3.2. Conformational analysis

In order to verify the 3D conformational arrangement of the peptides, CD and solution NMR spectra have been recorded. From CD spectra (Figure S1, Supplementary Material) analysis based on BestSel algorithm [34], peptides **2**, **3**, **4**, **6**, and **8** were found to be compatible with a β-hairpin folding (% of β-sheet structure > 30%; Table 2). In particular, **3** and **6** showed the highest β-sheet content (about 50%) in the series.

Starting from CD results, NMR analysis was performed on peptides **2**, **3**, **4**, **6**, and **8**. NMR spectra of all peptides in water solution showed a clear tendency of these peptides to adopt the β-hairpin structure (Tables S2–S7, Supplementary Material). In particular, a medium range NOE $H\alpha_i$-HN_{i+2} between residue 6 and residue 8 indicated the presence of a β-turn structure about residue 6–7; strong sequential NOEs in the segments 1–5 and 8–12 indicated that those regions are in extended conformation; moreover, inter-strands NOEs between residues 2–11 and 4–9 are clearly diagnostic of an antiparallel β-sheet (Table S8), thus defining an overall β-hairpin structure. Structure calculation was also performed on peptide **6**, which showed the most interesting binding properties (see below). The simulated annealing protocol based on the NMR constraints gave the structure displayed in Fig. 2. Peptide **6** shows a quite well-defined β-hairpin structure with a type I' β-turn on its tip. The four Trp residues form a zipper structure on one side of the β-hairpin while Gln (1,8), Arg (5,12) and Asn (3) are oriented on the other side forming a polar surface.

3.3. Interaction of β-hairpin-forming peptides with DNA oligomers

The study of peptide-DNA interactions was limited to those molecules able to form a β-hairpin structure (i.e. peptides **2**, **3**, **4**, **6**, and **8**), being it a favorable condition for DNA recognition and binding in the major groove. Such investigation concerned both the ds-oligonucleotide DNA1 containing the consensus target TAGA (ds-DNA1: 5′-GCGAG TAGA GC TTTTT GC TCTA CTCGC-3′) and DNA2 with a double mutation in the consensus sequence (ds-DNA2: 5′-GCGAG CACA GC TTTTT GC TGTG CTCGC-3′), as well as the calf thymus DNA (CT). To gain insights into the affinity of the investigated peptides towards such DNAs, methyl green displacement assays were performed. Briefly, this assay is based on the displacement of the methyl green (MG) from DNA upon addition of increasing amounts of a putative peptide-ligand. MG is a triphenylmethane dye able to bind to the DNA major groove with a stoichiometry of one molecule per thirteen nucleotides and showing a preferential binding for AT-rich regions [35,36] which is also the interaction site of the ARC repressor. MG is almost non-fluorescent when free in solution, while it becomes intensely fluorescent when bound to DNA [35]. Thus, a peptide-induced MG displacement produces a fluorescence intensity decrease which can be monitored as a function of the peptide concentration, thus allowing the evaluation of its relative binding affinity to the DNA under examination. We first performed a qualitative analysis of the MG displacement from DNA1 and DNA2 induced by addition of a molar excess of peptides **2**, **3**, **4**, **6**, and **8**. Results of these experiments, reported in Fig. 3, indicate that peptide **6**, which is characterized by one of the highest β-sheet content, was the most effective of the series in displacing MG from both DNA1 and DNA2.

Table 2
Percentage of secondary structure from CD spectra.

Peptide	Helix	β-sheet	Turn	Others
1	25.0	0.0	8.0	67.0
2	0.0	**30.9**	18.4	50.7
3	0.0	**51.2**	0.0	48.8
4	0.0	**32.4**	21.8	45.7
5	5.6	10.3	17.4	66.7
6	13.7	**47.1**	1.9	37.3
7	44.1	12.3	0.0	43.6
8	2.5	**37.1**	20.5	39.8
9	24.7	0.0	12.0	63.4
10	63.5	0.0	0.0	36.5

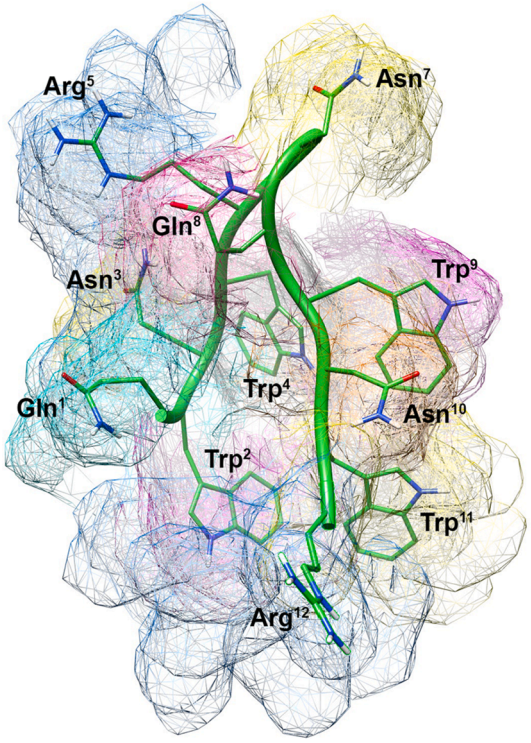

Fig. 2. Lowest energy conformer of peptide **6**. Backbone is evidenced as a ribbon. Side chains of the 10 lowest energy conformers are also shown as mesh surface. Surfaces are distinguished with different colors. (For interpretation of the references to color in this figure legend, the reader is referred to the web version of this article.)

Furthermore, in the case of DNA1 an almost selective MG displacement by the peptide **6** was observed. Indeed, except for peptide **2**, which induces a slight decrease in the MG fluorescence, all the other peptides do not produce any significant fluorescence variation with DNA1. On the contrary, in the case of DNA2 most of the investigated peptides (with the exception of **8**) seem to induce fluorescence changes in the MG-DNA complex, probably due to low-specific interaction with this DNA sequence. Again, peptide **6** is the most effective followed by peptide **2**. Interestingly, these two peptides share the same GN turn sequence (Table 1) suggesting that a type I' β-turn is the best suited within a β-hairpin peptide for the interaction with the DNA major groove.

Next, the affinity of **6** for DNA1 and DNA2 was evaluated by measuring the concentration of ligand required to decrease the fluorescence of the probe by 50% (DC_{50}) and determined after non-linear fitting of the displacement curve. Results of such experiments showed in Fig. 4 clearly revealed that the binding of peptide **6** does not strictly depend on the DNA sequence, since DC_{50} values of 25.5 (±1.3) and 12.8 (±0.7) μM were obtained for DNA1 and DNA2, respectively.

In the next step, it was studied if the interactions of designed peptides **2**, **3**, **4**, **6**, and **8** with DNA, when they occur, are specifically directed towards the major groove. Indeed, the possibility that these peptides could interact with DNA through intercalation or minor groove binding cannot be excluded a priori especially in the case of peptides **6** and **8** which have four tryptophan residues in their sequences [37]. Therefore, we decided to perform both ethidium bromide (EB) and Hoechst 33258 displacement assays. EB is known to intercalate between DNA base pairs [38], while Hoechst 33258 preferentially binds to the AT-rich regions of the minor groove of DNA [39]. The fluorescence intensity of both dyes increases remarkably upon binding to DNA, while a marked quenching of the fluorescence is expected if the peptide competes for the same binding site of the dye. In the case of EB displacement assay, none of the investigated peptides induced a significant displacement of EB from both DNA1 and DNA2, apart a very slight effect observed for peptide **8** (Fig. 5). To note that peptide **8** showed a very similar behavior with consensus DNA1 and mutated DNA2. These results would discard DNA intercalation of the peptides as the main DNA binding mode.

Regarding the Hoechst 33258 displacement assay, an almost negligible decrease of the fluorescence band of the DNA/dye complex was observed upon addition of a molar excess of peptides **3** and **4**, indicating that these peptides did not induce a significant displacement of Hoechst 33258 from both DNA1 and DNA2 (Fig. 6), discarding minor groove binding as principal DNA binding mode. On the other hand, peptides **2**, **6** and **8** induced both a slight increase in intensity and a blueshift of the fluorescence band of the DNA/dye complex both in the case of DNA1 and DNA2. This effect may arise from the spatial changes of the minor groove structure induced by the occupation of the major groove by peptides **2** or **6**, or by the weak intercalation ability of **8** as determined by MG and EB displacement experiments, respectively.

In order to obtain more information on the DNA binding process, we performed fluorescence anisotropy titrations by adding peptide **6** to a solution containing a tetramethylrhodamine (TMR)-labeled oligonucleotide, with both DNA1 or DNA2. The addition of **6** led to a progressive increase in the fluorescence anisotropy of the TMR label (Fig. 7). The data could be fitted to a simplified 1:1 binding model, calculating an apparent dissociation constant of 166 ± 23 μM for DNA1 and 236 ± 22 μM for DNA2.

3.4. Interaction of peptide 6 with polymeric calf thymus DNA

Since peptide **6** turned out to displace MG from the major groove of DNA1 and DNA2 in a similar manner, its interaction mode was further

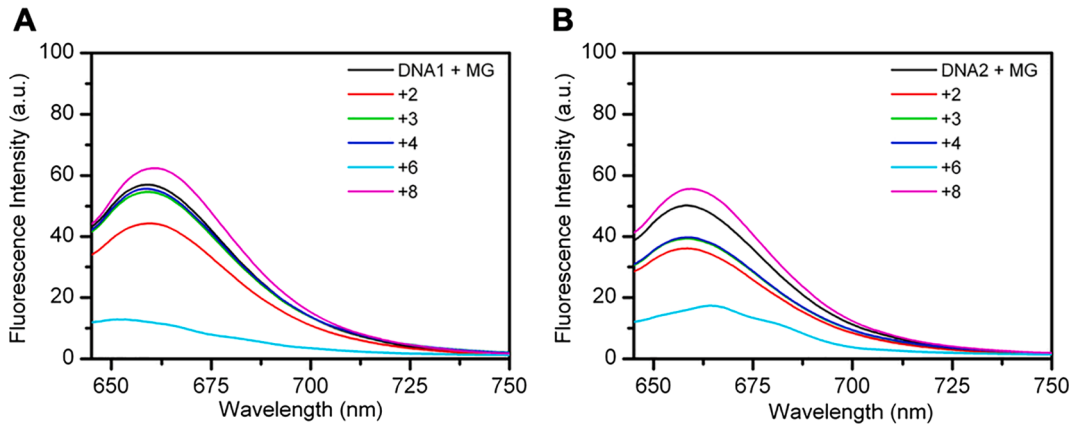

Fig. 3. Displacement of methyl green (MG) from (**A**) DNA1 and (**B**) DNA2 by the investigated peptides. (For interpretation of the references to color in this figure legend, the reader is referred to the web version of this article.)

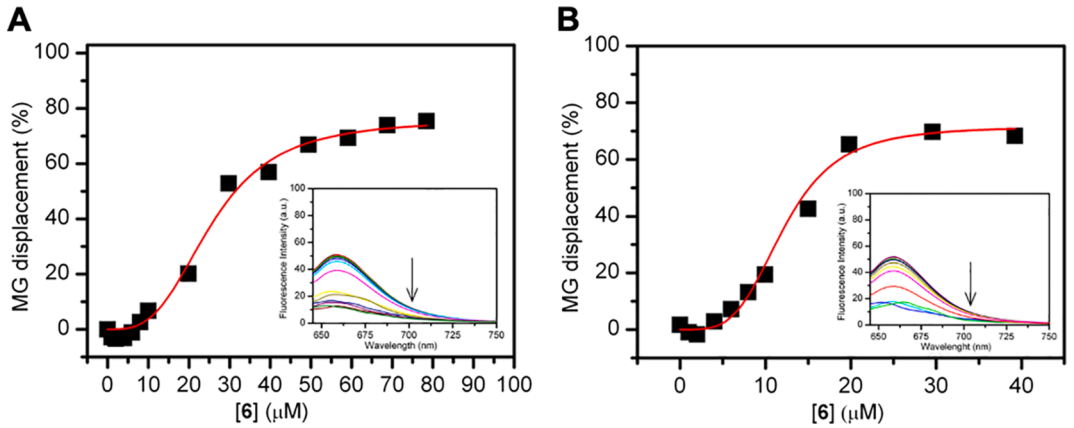

Fig. 4. Plots of peptide **6**-induced MG displacement for (**A**) DNA1 and (**B**) DNA2. Insets: fluorescence spectra in the presence of increasing amounts of **6**.

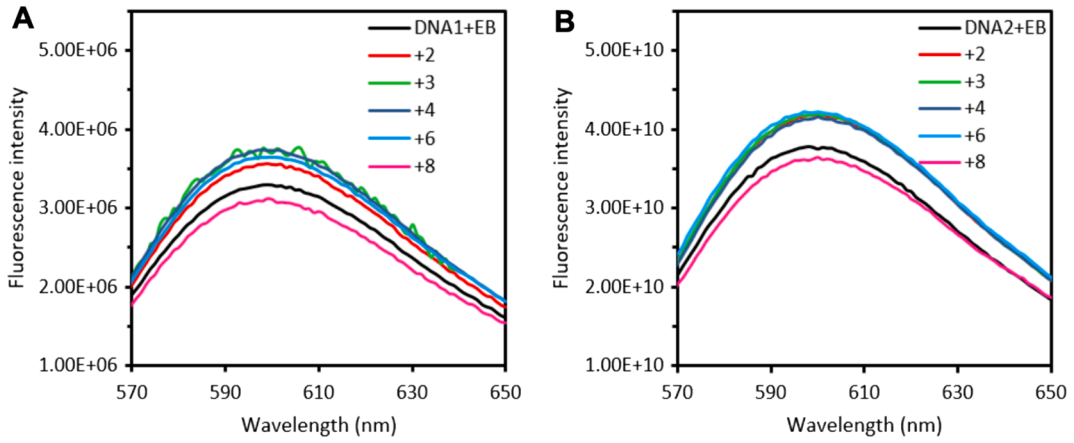

Fig. 5. Displacement of ethidium bromide (EB) from (**A**) DNA1 and (**B**) DNA2 by the investigated peptides.

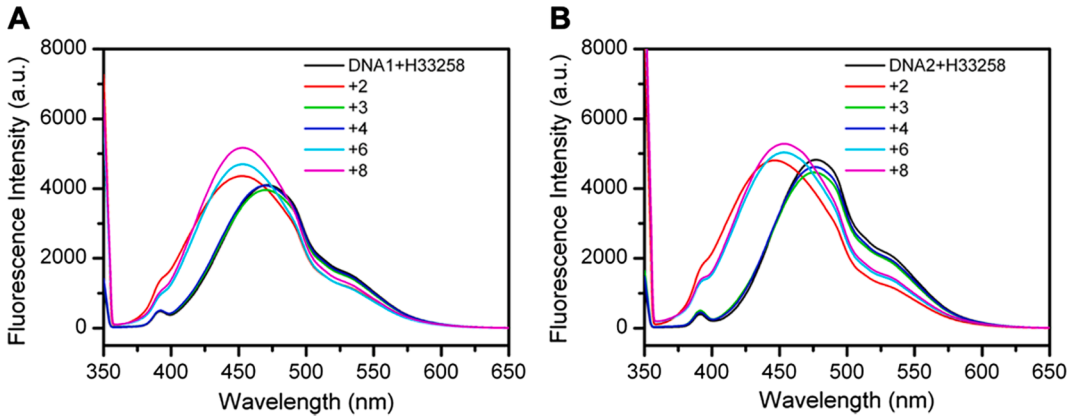

Fig. 6. Displacement of Hoechst 33,258 (H33258) from (**A**) DNA1 and (**B**) DNA2 by the investigated peptides.

investigated using double-stranded calf-thymus DNA (CT-DNA) as target. We first confirmed that peptide **6** was the best ligand of the series towards CT-DNA by performing a qualitative analysis of the MG displacement from this DNA induced by investigated peptides at high molar excess (Fig. 8A). Then, a titration experiment with stepwise addition of **6** to MG/CT-DNA complex was carried out. A concentration of 268 (±21) μM of **6** was required to displace 50% MG, thus indicating a markedly weaker affinity of such peptide for CT-DNA compared to DNA1 and DNA2 (Fig. 8B).

Alternative binding modes for peptide **6** to calf thymus DNA were investigated. Viscosity measurement is often regarded as an effective and accurate method to determine the binding mode between ligands and DNA. It is generally suggested that a classical intercalative binding mode causes a significant increase of DNA viscosity because the intercalative interaction requires the space of adjacent base pairs to be large enough to accommodate the bound small molecules and elongates the double helix [40]. However, for the electrostatic or groove binding, there is little effect on the viscosity of DNA. The viscosities of CT-DNA in Tris–HCl buffer solution (pH = 7.4) in the absence and presence of peptide **6** were measured and the results show that the viscosities of CT-

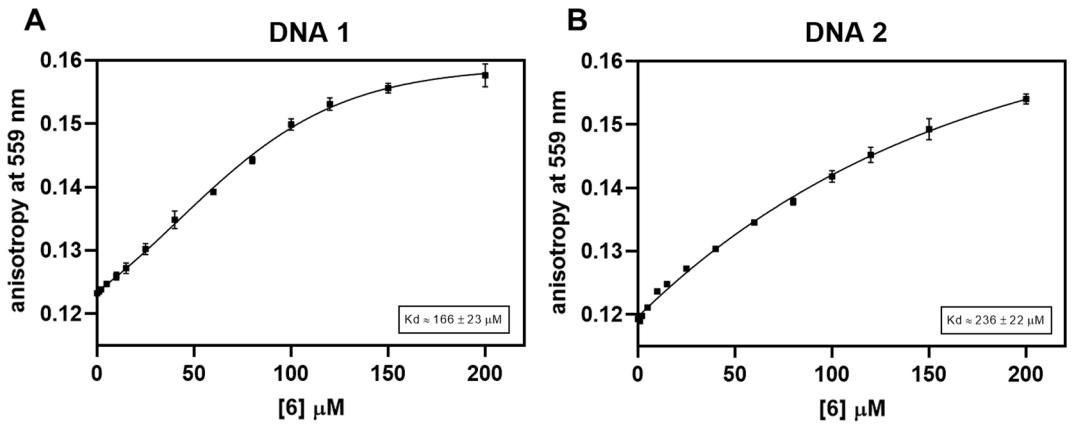

Fig. 7. Fluorescence anisotropy titration at 559 nm of a 1 μm solution of a tetramethylrhodamine-labeled oligonucleotide DNA1 (**A**) and DNA2 (**B**), with increasing concentrations of peptide **6**. The best fit to a 1:1 binding model is also shown. Experimental data correspond to the mean of three independent titration experiments.

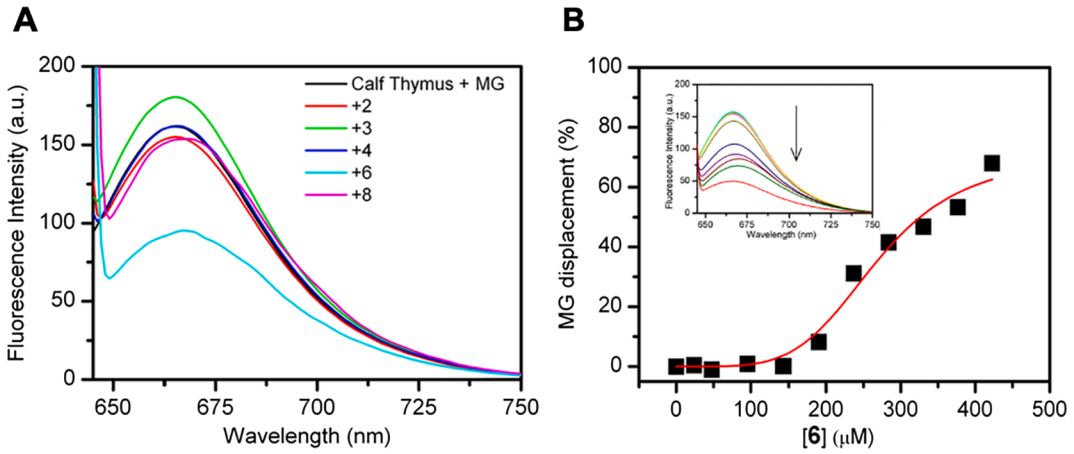

Fig. 8. (**A**) Displacement of methyl green (MG) from CT-DNA by the investigated peptides. (**B**) Plot of peptide **6**-induced MG displacement for calf thymus DNA. Inset: fluorescence spectra in the presence of increasing amounts of **6**. (For interpretation of the references to color in this figure legend, the reader is referred to the web version of this article.)

DNA almost do not change with the increasing concentration of peptide **6**, indicating that the binding mode of peptide **6** to CT-DNA is not the intercalative one (Supplementary Material, Figure S2).

3.5. *Interaction of peptide 6 with DNA1 and DNA2 by docking studies*

Interaction mode of peptide **6** with DNA1 and DNA2 was investigated by docking studies. NMR lowest energy structure of peptide **6** was docked with both DNA1 and DNA2 models. Docking procedures using the program AUTODOCK [28] clustered 100 poses in 24 clusters (10/100 poses in the first cluster) for **6**/DNA1 and 100 poses in 29 clusters for **6**/DNA2 complexes (11/100 poses in the first cluster). Statistics and energy terms are reported in Table S7 (Supplementary Material). Clearly, the high number of clusters indicate that docking did not provide a unique **6**/DNA1 or **6**/DNA2 complex (Fig. 9A,C) confirming that peptide **6** has not a sequence selectivity for DNA. Interestingly, peptide **6** interacts with the major groove of B-DNA according to the experimental displacement results. Moreover, the polar face of the hairpin is mainly involved in the interactions with the DNA while the Trp zipper has only a scaffold stabilization function. Fig. 9B and 9D show details on the peptide-base contacts of the lowest energy pose of **6**/DNA1 and **6**/DNA2 complexes, respectively. They include charge reinforced hydrogen bonds between guanidino and phosphate groups of Arg5 and A22, and Arg12 and A4; one hydrogen bond between Gln1 and A22; one hydrogen bond between Asn10 and T24 for **6**/DNA1 complex. Considering **6**/DNA2 complex, charge reinforced hydrogen bonds between Arg5 and *C*2, Arg12 with A9 and G10; one hydrogen bond between Asn10 and T19; one hydrogen bond between Gln1 and G1 were observed. To note that the free energy of binding of **6**/DNA1 is higher than **6**/DNA2 complex (−4.29 vs −7.99 kcal/mol, Table S7). Moreover, considering the lowest energy poses, peptide **6** does not interact within the TAGA box in the **6**/DNA1 complex, while it displays various contacts with the corresponding CACA box in the **6**/DNA2 complex. These findings can give the key to understanding the observed lower affinity of peptide **6** for DNA1 compared to DNA2.

4. Conclusion

The design of peptides with a well-defined structure as ARC mimetics is an appealing task in the field of medicinal chemistry due to its novelty and specificity, because the binding to the DNA is made by a β-sheet domain, which is peculiar, being alpha helix often used for this process. In this paper, we have designed a series of linear and cyclic β-hairpin dodeca-peptides with the aim to mimic the 3D structure of the ARC β-sheet region interacting with DNA; among them, peptides **2**, **3**, **4**, **6** and **8** display a β-hairpin structure. We found that one of our peptides, peptide **6**, is able to bind DNA, albeit without sequence selectivity. However, it shows a topological selectivity since it binds to the major groove of the DNA which, interestingly, is the interaction site of ARC and many other DNA-binding proteins. Moreover, we found that a type

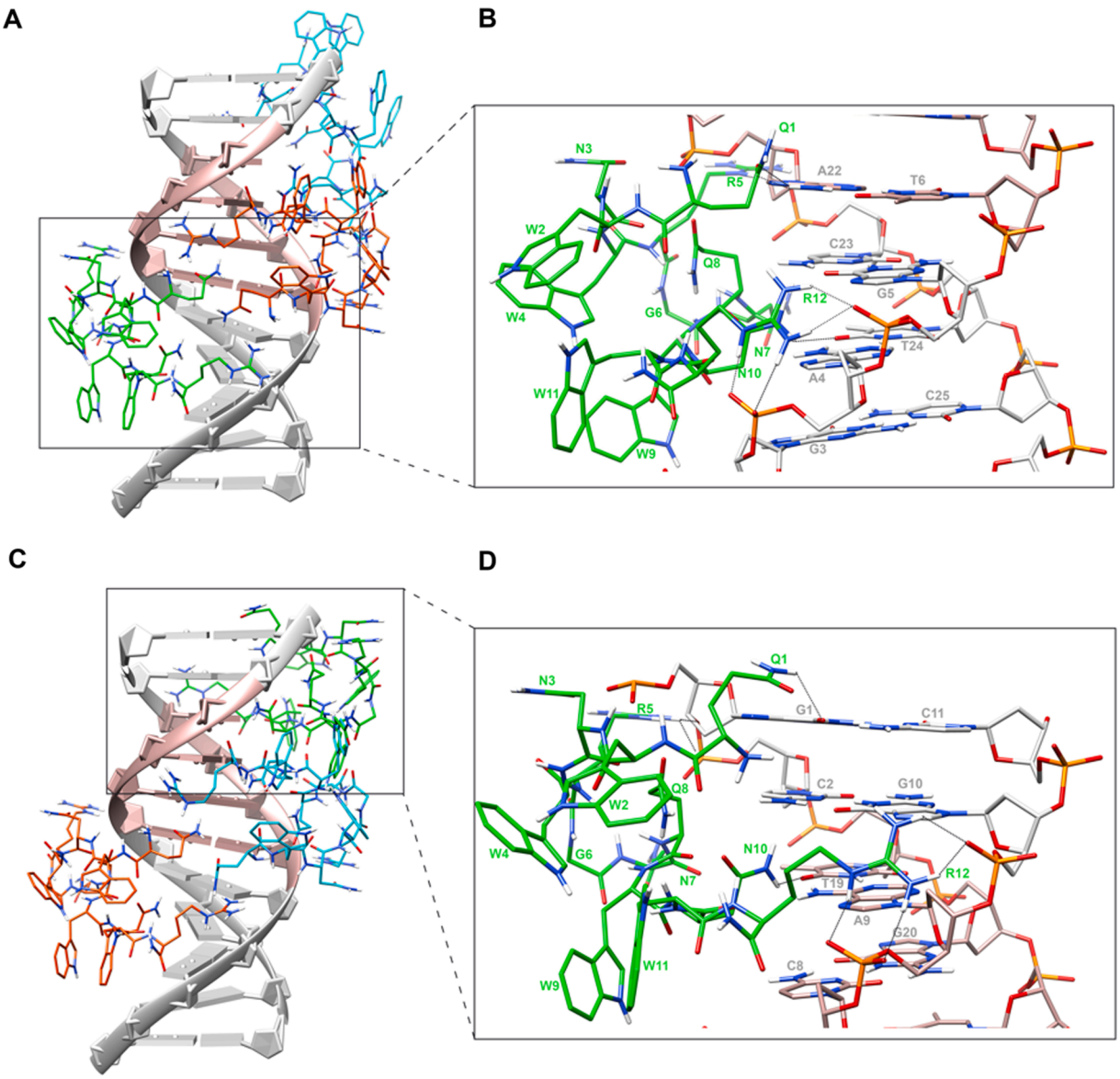

Fig. 9. (**A**) DNA1 or (**C**) DNA2 model in complex with peptide **6**. The three lowest energy poses of each docking calculation are shown (carbon atoms of the absolute lowest pose are shown in green). DNA backbone is represented as gray ribbon, bases are displayed as slab. TAGA or CACA box are evidenced in pink. (**B**) Zoom of the peptide **6** lowest energy pose interacting with DNA1 or (**D**) DNA2. Hydrogen bonds are represented with dashed lines. Color codes: polar hydrogen, white; nitrogen, blue; oxygen, red; phosphorous, yellow. Non-polar hydrogens are not shown for clarity. (For interpretation of the references to color in this figure legend, the reader is referred to the web version of this article.)

I' β-harpin folding pattern is a favorite peptide structure for interaction with the B-DNA major groove. Docking investigation gave atomic details about the interactions between peptide **6** and the considered oligonucleotides. Further work is under way in our laboratory to develop, starting from peptide **6**, analogs with B-DNA sequence selectivity.

Declaration of Competing Interest

The authors declare that they have no known competing financial interests or personal relationships that could have appeared to influence the work reported in this paper.

Acknowledgment

This work was supported by the Regione Campania – POR Campania FESR 2014/2020 "Combattere la resistenza tumorale: piattaforma integrata multidisciplinare per un approccio tecnologico innovativo alle oncoterapie – Campania Oncoterapie" (B61G18000470007).

Appendix A. Supplementary material

Supplementary data to this article can be found online at https://doi.org/10.1016/j.bioorg.2021.104836.

References

[1] F. Spitz, E.E.M. Furlong, Transcription factors: from enhancer binding to developmental control, Nat. Rev. Genet. 13 (2012) 613–626, https://doi.org/10.1038/nrg3207.
[2] M. Eugenio Vázquez, A.M. Caamaño, J.L. Mascareñas, From transcription factors to designed sequence-specific DNA-binding peptides, Chem. Soc. Rev. 32 (2003) 338–349, https://doi.org/10.1039/b206274g.
[3] K.L. Knight, J.U. Bowie, A.K. Vershon, R.D. Kelley, R.T. Sauer, A.K. Vershong, R. T. Sauer, A.K. Vershon, R.D. Kelley, R.T. Sauer, A.K. Vershong, R.T. Sauer, The arc and Mnt repressors, J. Biol. Chem. 264 (1989) 3639–3642.
[4] D. Hanahan, R.A. Weinberg, Hallmarks of cancer: the next generation, Cell. 144 (2011) 646–674, https://doi.org/10.1016/j.cell.2011.02.013.

[5] P. Panegyres, J.T. Burchell, Prion diseases: immunotargets and therapy, ImmunoTargets Ther. 5 (2016) 57–68, https://doi.org/10.2147/itt.s64795.
[6] M.M. Evers, L.J.A. Toonen, W.M.C. van Roon-Mom, Antisense oligonucleotides in therapy for neurodegenerative disorders, Adv. Drug Deliv. Rev. 97 (2015) 90–103, https://doi.org/10.1016/j.addr.2015.03.008.
[7] L. Dostál, R. Misselwitz, H. Welfle, Arc repressor - operator DNA interactions and contribution of Phe10 to binding specificity, Biochemistry. 44 (2005) 8387–8396, https://doi.org/10.1021/bi0476073.
[8] E. Pazos, J. Mosquera, M.E. Vázquez, J.L. Mascareñas, DNA recognition by synthetic constructs, ChemBioChem. 12 (2011) 1958–1973, https://doi.org/10.1002/cbic.201100247.
[9] D. Bhunia, P. Mondal, G. Das, A. Saha, P. Sengupta, J. Jana, S. Mohapatra, S. Chatterjee, S. Ghosh, Spatial position regulates power of tryptophan: discovery of a major-groove-specific nuclear-localizing, cell-penetrating tetrapeptide, J. Am. Chem. Soc. 140 (2018) 1697–1714, https://doi.org/10.1021/jacs.7b10254.
[10] O.S.L. Gonçalves, G. Christiansen, A. Holm, B. Herrmann, M. Klintstedt, S. B. Petersen, S. Birkelund, The repeated 36 amino acid motif of Chlamydia trachomatis Hc2 protein binds to the major groove of DNA, Res. Microbiol. 170 (2019) 256–262, https://doi.org/10.1016/j.resmic.2019.08.002.
[11] A. Stefanucci, J. Mosquera, E. Vázquez, J.L. Mascareñas, E. Novellino, A. Mollica, Synthesis, characterization, and DNA binding profile of a macrocyclic β-sheet analogue of ARC protein, ACS Med. Chem. Lett. 6 (2015) 1220–1224, https://doi.org/10.1021/acsmedchemlett.5b00363.
[12] M.T. Pastor, M.L. De La Paz, E. Lacroix, L. Serrano, E. Pérez-Payá, Combinatorial approaches: a new tool to search for highly structured β-hairpin peptides, Proc. Natl. Acad. Sci. U. S. A. 99 (2002) 614–619, https://doi.org/10.1073/pnas.012583999.
[13] A.M.C. Marcelino, L.M. Gierasch, Roles of β-turns in protein folding: from peptide models to protein engineering, Biopolymers. 89 (2008) 380–391, https://doi.org/10.1002/bip.20960.
[14] J. Amato, G. Miglietta, R. Morigi, N. Iaccarino, A. Locatelli, A. Leoni, E. Novellino, B. Pagano, G. Capranico, A. Randazzo, Monohydrazone based G-quadruplex selective ligands induce DNA damage and genome instability in human cancer cells, J. Med. Chem. 63 (2020) 3090–3103, https://doi.org/10.1021/acs.jmedchem.9b01866.
[15] T.L. Hwang, A.J. Shaka, Water suppression that works. excitation sculpting using arbitrary wave-forms and pulsed-field gradients, J. Magn. Reson. - Ser. A. 112 (1995) 275–279, https://doi.org/10.1006/jmra.1995.1047.
[16] U. Piantini, O.W. Sørensen, R.R. Ernst, Multiple quantum filters for elucidating NMR coupling networks, J. Am. Chem. Soc. 104 (1982) 6800–6801, https://doi.org/10.1021/ja00388a062.
[17] D. Marion, K. Wüthrich, Application of phase sensitive two-dimensional correlated spectroscopy (COSY) for measurements of 1H–1H spin-spin coupling constants in proteins, Biochem. Biophys. Res. Commun. 113 (1983) 967–974, https://doi.org/10.1016/0006-291X(83)91093-8.
[18] K. Wüthrich, NMR of proteins and nucleic acids, New York (1986), https://doi.org/10.1039/b618334b.
[19] L. Braunschweiler, R.R. Ernst, Coherence transfer by isotropic mixing: Application to proton correlation spectroscopy, J. Magn. Reson. 53 (1983) 521–528, https://doi.org/10.1016/0022-2364(83)90226-3.
[20] J. Jeener, B.H. Meier, P. Bachmann, R.R. Ernst, Investigation of exchange processes by two-dimensional NMR spectroscopy, J. Chem. Phys. 71 (1979) 4546, https://doi.org/10.1063/1.438208.
[21] D.J. States, R.A. Haberkorn, D.J. Ruben, A two-dimensional nuclear overhauser experiment with pure absorption phase in four quadrants, J. Magn. Reson. 48 (1982) 286–292, https://doi.org/10.1016/0022-2364(82)90279-7.
[22] C. Bartels, T. he Xia, M. Billeter, P. Güntert, K. Wüthrich, The program XEASY for computer-supported NMR spectral analysis of biological macromolecules, J. Biomol. NMR. 6 (1995) 1–10, https://doi.org/10.1007/BF00417486.
[23] P. Güntert, L. Buchner, Combined automated NOE assignment and structure calculation with CYANA, J. Biomol. NMR. 62 (2015) 453–471, https://doi.org/10.1007/s10858-015-9924-9.
[24] J.R. Maple, U. Dinur, A.T. Hagler, Derivation of force fields for molecular mechanics and dynamics from ab initio energy surfaces, Proc. Natl. Acad. Sci. 85 (1988) 5350–5354, https://doi.org/10.1073/pnas.85.15.5350.
[25] E.F. Pettersen, T.D. Goddard, C.C. Huang, G.S. Couch, D.M. Greenblatt, E.C. Meng, T.E. Ferrin, UCSF chimera - a visualization system for exploratory research and analysis, J. Comput. Chem. 25 (2004) 1605–1612, https://doi.org/10.1002/jcc.20084.
[26] P. Kuzmič, DynaFit–a software package for enzymology, Methods Enzymol. 467 (2009) 247–280, https://doi.org/10.1016/S0076-6879(09)67010-5.
[27] P. Kuzmic, Program DYNAFIT for the analysis of enzyme kinetic data: application to HIV proteinase, Anal Biochem. 237 (1996) 260–273, https://doi.org/10.1006/abio.1996.0238.
[28] G.M. Morris, R. Huey, W. Lindstrom, M.F. Sanner, R.K. Belew, D.S. Goodsell, A. J. Olson, AutoDock4 and AutoDockTools4: automated docking with selective receptor flexiblity, J. Comput. Chem. 30 (2009) 2785–2791, https://doi.org/10.1002/jcc.21256.
[29] L. Wu, D. Mcelheny, V. Setnicka, J. Hilario, T.A. Keiderling, Role of different β-turns in β-hairpin conformation and stability studied by optical spectroscopy, Proteins Struct. Funct. Bioinforma. 80 (2012) 44–60, https://doi.org/10.1002/prot.23140.
[30] C.M. Santiveri, J. Santoro, M. Rico, M.A. Jiménez, Factors involved in the stability of isolated β-sheets: turn sequence, β-sheet twisting, and hydrophobic surface burial, Protein Sci. 13 (2004) 1134–1147, https://doi.org/10.1110/ps.03520704.
[31] L. Martínez, A. Sampedro, E. Sanna, A. Costa, C. Rotger, Synthesis and conformational studies of peptido-squaramide foldable modules: a new class of turn-mimetic compounds, Org. Biomol. Chem. 10 (2012) 1914–1921, https://doi.org/10.1039/c2ob06715c.
[32] A. Stefanucci, R. Costante, G. Macedonio, S. Dvoracsko, A. Mollica, Cysteine-, methionine- and seleno-cysteine-proline chimeras: synthesis and their use in peptidomimetics design, Curr. Bioact. Compd. 12 (2016) 200–206, https://doi.org/10.2174/1573407212666160511162915.
[33] A.G. Cochran, N.J. Skelton, M.A. Starovasnik, Tryptophan zippers: stable, monomeric β-hairpins, Proc. Natl. Acad. Sci. U. S. A. 98 (2001) 5578–5583, https://doi.org/10.1073/pnas.091100898.
[34] A. Micsonai, F. Wien, L. Kernya, Y.H. Lee, Y. Goto, M. Réfrégiers, J. Kardos, Accurate secondary structure prediction and fold recognition for circular dichroism spectroscopy, Proc. Natl. Acad. Sci. U.S.A. 112 (2015) E3095–3103, https://doi.org/10.1073/pnas.1500851112.
[35] A.K. Krey, F.E. Hahn, Studies on the Methyl Green-DNA complex and its dissociation by drugs, Biochemistry. 14 (1975) 5061–5067, https://doi.org/10.1021/bi00694a005.
[36] S.K. Kim, B. Nordén, Methyl green a DNA major-groove binding drug, FEBS Lett. 315 (1993) 61–64, https://doi.org/10.1016/0014-5793(93)81133-K.
[37] M.R. Rajeswari, T. Montenay-Garestier, C. Helene, Does tryptophan intercalate in DNA? a comparative study of peptide binding to alternating and nonalternating A·T sequences, Biochemistry. 26 (1987) 6825–6831, https://doi.org/10.1021/bi00395a036.
[38] P.O. Vardevanyan, A.P. Antonyan, M.A. Parsadanyan, H.G. Davtyan, A. T. Karapetyan, The binding of ethidium bromide with DNA: interaction with single- and double-stranded structures, Exp. Mol. Med. 35 (2003) 527–533, https://doi.org/10.1038/emm.2003.68.
[39] J.A.C. Chen, R.A. Jockusch, Protomers of DNA-binding dye fluoresce different colours: intrinsic photophysics of Hoechst 33258, Phys. Chem. Chem. Phys. 21 (2019) 16848–16858, https://doi.org/10.1039/c9cp02421b.
[40] Z. Molphy, D. Montagner, S.S. Bhat, C. Slator, C. Long, A. Erxleben, A. Kellett, A phosphate-targeted dinuclear Cu(II) complex combining major groove binding and oxidative DNA cleavage, Nucleic Acids Res. 46 (2018) 9918–9931, https://doi.org/10.1093/nar/gky806.